Nuclear Inst. and Methods in Physics Research, A 902 (2018) 76–82

Contents lists available at ScienceDirect

Nuclear Inst. and Methods in Physics Research, A

journal homepage: www.elsevier.com/locate/nima

Effects of capacitance ratio on the image linearity of capacitive division image readout

Fanpu Lei [a,b,*], Yonglin Bai [a], Bingli Zhu [a], Bo Wang [a], Xiaohong Bai [a], Xun Hou [a]

[a] State Key Laboratory of Transient Optics and Photonics, Xi'an Institute of Optics and Precision Mechanics (XIOPM), Chinese Academy of Sciences (CAS), Xi'an 710119, China

[b] University of Chinese Academy of Sciences (CAS), Beijing 100049, China

ARTICLE INFO

Keywords:
Capacitive anode
Charge division
Image linearity

ABSTRACT

Capacitive division readout anode has the advantages of simple manufacture technology and high spatial resolution. Linearity of the restored image is limited by the relationship between the values of C (charge divide capacitor), C_s (parasitic capacitor), C_d (capacitor introduced by diagonal electrode) and C_p (perimeter capacitor). This paper describes a discrete capacitance matrix to investigate the dependence of image linearity on capacitor ratios, including C/C_s, C/C_d and(N-1)C/C_p (N is the number of nodes in each row of the capacitance matrix). Results presents that image nonlinearity varies monotonically with C/C_s, C/C_d and(N-1)C/C_p. The effect of these capacitors on the linearity of image can be negligible when C/C_s is greater than 100, C/C_d is greater than 10 and (N-1)C/C_p is smaller than 0.1. The reliability of the simulation results is verified by experiments. The RMS nonlinearity of capacitive anode is expected to less than 0.71%.

1. Introduction

The earth's ionosphere inevitably affects the quality and accuracy of Global Navigation Satellite Systems (GNSS). Researchers found that the intensity of 135.6 nm airglow in the ionosphere can be used to determine the refractive and reflective index of earth's ionosphere, which are parameters affecting the GNSS [1–3]. Therefore observing the nightglow of 135.6 nm with a satellite-borne ultraviolet imaging detector has great significance to the GNSS.

MCP detector could be used to observe the nightglow of 135.6 nm due to its high detection sensitivity and low background noise. Charge division position readout for MCP detectors has been traditionally carried out, such as resistive anode [4] and wedge-and-strip anode (WSA) [5], using only three or four output channels. However, the resistive anode is difficult to balance between spatial resolution and count rate caused by Johnson noise and pulse processing time. The WSA suffers relatively large input capacitance causing deterioration of spatial resolution. Devices such as the Vernier anode [6] and cross-strip anode [7] have sought to overcome these limitations, but at the expense of higher complexity.

Image readout based on the concept of capacitive charge division has been described by Gott [8]. It has not been greatly utilized until Lapington [9,10] proposed the idea of Capacitive Division Image Readout (C-DIR). The electronic configuration of a capacitive charge division network as shown in Fig. 1 constitutes of four types of capacitors: main charge division capacitors C providing the signal path, diagonal capacitors C_d, perimeter capacitors C_p and electrode parasitic capacitors C_s (only a small part of C_s is shown for simplification). As the event charge deposits on resistive layer, signal transient is coupled through a dielectric to the capacitive readout and is divided via C, C_d, C_p and C_s to four measurement nodes at four corners of the readout. The event coordinate is then calculated by:

$$x = \frac{Q_B + Q_C}{Q_A + Q_B + Q_C + Q_D} \quad (1)$$

$$y = \frac{Q_A + Q_B}{Q_A + Q_B + Q_C + Q_D} \quad (2)$$

where Q_A, Q_B, Q_C, and Q_D correspond to the charge collected at A, B, C and D output nodes respectively.

Since the capacitive charge division readout is a passive circuit made by capacitors only, the capacitive anode has no bandwidth limitation [11] and low Johnson (due to the resistive nature of resistive anode) and partition noise (due to charge collection amongst discrete electrodes) [12], producing excellent spatial resolution.

* Correspondence to: State Key Laboratory of Transient Optics and Photonics, Xi'an Institute of Optics and Precision Mechanics (XIOPM), Chinese Academy of Sciences (CAS), No.17 Xinxi Road, New Industrial Park, Xi'an Hi-Tech Industrial Development Zone, Xi'an, Shaanxi Province, China.
E-mail address: leifanpu@opt.ac.cn (F. Lei).

https://doi.org/10.1016/j.nima.2018.06.030
Received 3 April 2018; Received in revised form 5 June 2018; Accepted 11 June 2018
Available online 19 June 2018
0168-9002/

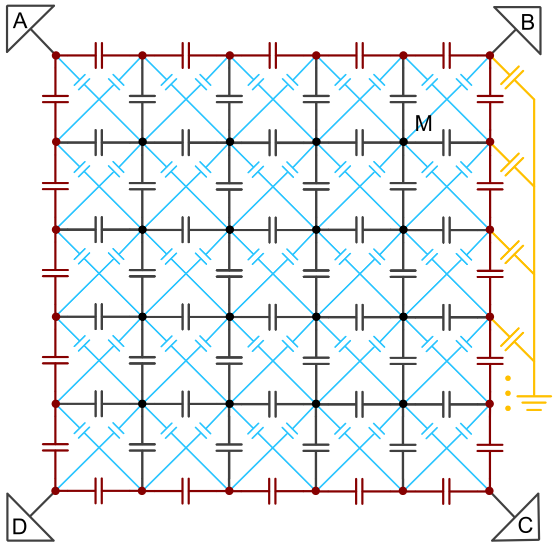

Fig. 1. Electronic configurations of capacitive anode. C, C_d, C_p and C_s are represented by black lines, blue lines, red lines and yellow lines, respectively. A, B, C and D are corner contacts used to obtain position information. M is the position of induced signal to be used in the calculation in Section 3.1. (For interpretation of the references to color in this figure legend, the reader is referred to the web version of this article.)

Capacitive anode has been successfully applied and achieved a spatial resolution of 150 μm [9]. The available simulation and experimental data to explore the relationship among the four types of capacitors to minimize image nonlinearity, however, is sparse. In this paper, a realistic model is described and analyzed based on the nodal analysis. Effect of the relevant capacitance ratio on position linearity is studied quantitatively. This allows for a determination of the optimum anode parameters to achieve minimum position nonlinearity.

2. Theory and simulation details

The purpose of anode detector is to recover the incident position of the photoelectrons generated by photons. The calculation formula is as above. The reason for nonlinearity is that the calculations of x and y have deviations, that is, Q_A, Q_B, Q_C and Q_D are different from the ideal case. The charge uncertainties caused by the capacitance ratio in the four outputs are uncorrelated. Thus the uncertainty in x and y can be derived using propagation of errors by measuring the uncertainties in Q_A, Q_B, Q_C, Q_D:

$$\sigma_x^2 = \left(\frac{\partial x}{\partial Q_A}\right)^2 \sigma_{Q_A}^2 + \left(\frac{\partial x}{\partial Q_B}\right)^2 \sigma_{Q_B}^2 + \left(\frac{\partial x}{\partial Q_C}\right)^2 \sigma_{Q_C}^2 + \left(\frac{\partial x}{\partial Q_D}\right)^2 \sigma_{Q_D}^2 \quad (3)$$

$$\sigma_y^2 = \left(\frac{\partial y}{\partial Q_A}\right)^2 \sigma_{Q_A}^2 + \left(\frac{\partial y}{\partial Q_B}\right)^2 \sigma_{Q_B}^2 + \left(\frac{\partial y}{\partial Q_C}\right)^2 \sigma_{Q_C}^2 + \left(\frac{\partial y}{\partial Q_D}\right)^2 \sigma_{Q_D}^2. \quad (4)$$

The capacitive anode is modeled as a series of discrete capacitors connected as Fig. 1 with N nodes in each row or column. Charge induction via the dielectric substrate couples the signal to any node on the capacitive anode and the charge induction path is called input branch. The four signal output paths are called output branches. (In practical applications, the charge is induced to several nodes so the spatial resolution of the anode is not limited by the size of the anode capacitor. According to the superposition principle of conductor system charge distribution, the effect of charge induced to multiple nodes is the same as the superposition effect of the corresponding charge induced to each node separately. In the next simulations, it is assumed that the charge is induced to one node each time. It has no side effect upon the centroid finding. In addition under this circumstance the theoretical incident position of the charge is precisely the node, which is convenient for the calculation of the image nonlinearity.)

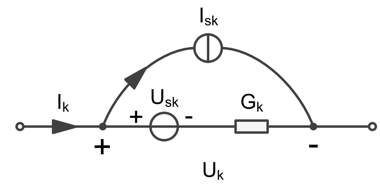

Fig. 2. Universal resistance branch.

Assume that the four output ports and the charge input port are connected to the same node through different branches to meet the Kirchhoff's current law (KCL). Under this assumption, the number of nodes and branches in a circuit like Fig. 1 will be:

$$n_n = N^2 + 1 \quad (5)$$

$$n_b = 2 \cdot N \cdot (N-1) + 2 \cdot (N-1)^2 + N^2 + 5 \quad (6)$$

where $2 \cdot N \cdot (N-1)$ represents the horizontal and vertical branches, $2 \cdot (N-1)^2$ represents the diagonal branches, N^2 represents the branches from each node to the ground and 5 is the input and output branches. Then according to the KCL, we could derive:

$$AI_b = 0 \quad (7)$$

where A is the $(n_n - 1) \times n_b$ incidence matrix, which has one row for each branch and one column for any $n_n - 1$ nodes in the n_n nodes. The element $A_{i,j}$ in row i and column j is 1 if the current in branch b_j leaves node n_i, −1 if b_j enters n_i, and 0 if b_j and n_i are not related. I_b is a $n_b \times 1$ column matrix, and each element of the matrix corresponds to the current on the corresponding branch. According to the Kirchhoff's voltage law (KVL), we could derive:

$$U_b = A^T U_n \quad (8)$$

where U_b is a $n_b \times 1$ column matrix, representing the potential difference between the two nodes of each branch. U_n is a $(n_n - 1) \times 1$ column matrix, representing the voltage of the corresponding node. The universal resistance branch, shown in Fig. 2 has voltage source and resistance connected in series, and in parallel with current source. Based on the constitutive relation, we can get:

$$I_b = GU_b + I_s - GU_s \quad (9)$$

where G is the conductance matrix whose diagonal element equals to the conductance of each branch and the rest is zero. I_s and U_s, $n_b \times 1$ column matrix, represent the independent current source matrix and independent voltage source matrix respectively.

I_b could be calculated according to Eq. (5) through Eq. (9). Since charge is the integral of current over time, the coordinate of incident charge can be obtain by Eqs. (1) and (2) using the known current of the output branches. Since Eqs. (7) to (9) are all matrix operations, and the total number of branches n_b is usually very large, the calculations in this paper are all completed using the mathematics software MATLAB developed by MathWorks [13].

3. Results and discussions

The dependence of linearity of the recovered image on the charge division capacitors is related to the capacitance ratio and independent of the specific capacitor [14]. In this section the relationship between the